Collective synthesis and dissociation of soliton molecules in parallel optical-soliton reactors

Wenbin He (wenbin.he@mpl.mpg.de)
wenbin.he@mpl.mpg.de
Meng Pang
Max Planck Institute for the Science of Light
Dung-Han Yeh
Max Planck Institute for the Science of Light
Jiapeng Huang
Max Planck Institute for the Science of Light
Philip Russell
Max Planck Institute for the Science of Light https://orcid.org/0000-0002-8972-2477

Article

Keywords: soliton molecules, lasers, light fields, optical control, optical resonators

Posted Date: August 21st, 2020

DOI: https://doi.org/10.21203/rs.3.rs-57272/v1

Abstract

Mode-locked lasers have been widely used to explore interactions between optical solitons, including bound-soliton states that may be regarded as "photonic molecules". Conventional mode-locked lasers normally however host at most only a few solitons, which means that stochastic behaviours involving large numbers of solitons cannot easily be studied under controlled experimental conditions. Here we report the use of an optoacoustically mode-locked fibre laser to create hundreds of temporal traps or "reactors" in parallel, within each of which multiple solitons can be isolated and controlled both globally and individually using all-optical method. We achieve on-demand synthesis and dissociation of soliton molecules within these reactors, in this way unfolding a novel panorama of diverse dynamics in which the statistics of multi-soliton interactions can be studied. The results are of crucial importance in understanding dynamical soliton interactions, and may motivate potential applications for all-optical control of ultrafast light fields in optical resonators.

Introduction

Temporal optical solitons in optical fibres, since first observed decades ago[1], have attracted widespread interests and stimulated foresights in applications that would potentially revolutionize optical communication[2] and computations[3] in the light of their particle-like properties. Naturally, interactions between solitons in fibres[4,5] were brought under spotlight as critical limitations or mechanisms in these applications, leading to a heap of progresses since 1980s. The studies on soliton interactions continue to date and are currently experiencing a vibrant renaissance, partly due to developments of the time-stretched dispersive Fourier transform (DFT) method[6] which facilitates resolving of transient soliton dynamics, as well as due to trending focuses on soliton microresonators[7–9] which, as novel platforms, advance rapidly toward chip-scale integration. In parallel, many light-matter analogies have been suggested for multi-soliton complexes bound by soliton interactions[10–16], epitomized by the “soliton molecules”[17,18] which refers to closely bound solitons through direct interactions[19–22]. Reminiscent of chemical molecules synthesized from single atoms, optical soliton molecules behave like a single entity while displaying complex internal dynamics[11,12,23–26], and have attracted considerable interest both in fundamental nonlinear physics and refreshed application promises such as ultrafast lasers[10,27,28], spectroscopy[29] ,optical communications[2,30] and all-optical information processing[3,12,14,31].

The light-matter analogy hold by soliton molecules can hardly, however, hide behind an obvious disparity: whereas chemical molecules usually participate in huge numbers in dynamic processes such as chemical reaction, soliton molecules have mostly been investigated as single entities. The cavity of mode-locked lasers, which has been routinely used as a platform for investigating complex soliton dynamics[10,11,23,32–34], are conventionally able to host only few solitons generated out of random excitations[24,25]. These solitons are actually results of double balances, with gain and loss in addition to nonlinearity and dispersion, known as dissipative solitons[10]. To understand the stochasticity of their complex interactions[24,32,35–37] in the nonlinear dissipative system from a collective level, large numbers

of solitons and soliton complexes with controllable interactions are demanded, which, however, has long been challenging in the experiments[12,14,15]. In particular, as analogous with chemical reactions between atoms, the synthesis of soliton-molecules from single solitons, and their dissociation into single solitons[10] has not yet been experimentally demonstrated in a fully controlled manner so far.

The physical scale of a mode-locked fibre laser is typically many times longer than an individual soliton, permitting in principle the coexistence of very large numbers of solitons and soliton molecules. In practice, however, uncontrollable drifting and collisions caused by noise[5,36,38,39], together with intrinsic group velocity differences between solitonic elements[40–42], has greatly limited the flexibility of mode-locked lasers as hosts for large solitonic structures. We have previously reported that the optomechanical lattice created in a mode-locked fibre laser[14] by a short length of photonic crystal fibre (PCF)[43] can synchronize the velocities of intra-cavity solitonic elements through long-range soliton interactions. Several solitonic elements can be temporally isolated and stably trapped within each time-slot of the optomechanical lattice, forming a stable supramolecular structure[15]. In this work we report that the consecutive time-slots of the optomechanical lattice can function as parallel soliton “reactors” which can be controlled with all-optical techniques, echoing experiments on controlling chemical reactions by atomic manipulation[44]. By deliberately initiating the formation and dissociation of soliton molecules in these parallel reactors globally and individually using a variety of all-optical methods, we are able to uncover previously unexplored stochastic aspects of soliton-soliton interactions. The build-up of a stable soliton molecule, observed in the experiments, generally requires multiple collisions[8,19,24,25] before the eventual establishment of stable soliton-soliton spacing and phase. In contrast, the break-up of soliton molecules can occur in many difference ways. We found that soliton motions during these two processes follow similar random-walk-like trajectories, accompanied with occasional radical repulsions and metastable states. While the statistical analysis on these processes reveals that the reaction rates of optical solitons follow classical theory of chemical kinetics, the first demonstration of fully-controlled switching between different multi-soliton states in parallel optical-soliton reactors suggests many potential applications in information storage, data processing and logical operations using optical-soliton bits[12,14,30,31].

System Configuration

The optoacoustically mode-locked fibre laser built to host and control the parallel optical-soliton reactors is briefly sketched in Fig. 1a (see details in Supplementary Information (SI) Section I). A 2-m-long solid-core PCF (core-structure in Fig. 1b) supporting an R_{01}-like mechanical resonance[43] at 1.887 GHz is inserted into an Er-doped fibre laser cavity (Fig. 1c). The optically-driven acoustic vibration in the PCF core divides the ~ 20 m cavity (~ 104 ns round-trip time) into 195 time-slots ~ 532 ps wide (one acoustic cycle), creating a self-organized and self-stabilized optomechanical lattice[14]. At pump powers above 600 mW, this lattice can be adjusted to host a variety of solitonic supramolecules[15]. Each time-slot of the optomechanical lattice, functioning as a potential well, can stably trap one or more solitons bound by

long-range and/or short-range forces (see Fig. 1d), while the entire structure can accommodate a large population of solitons and soliton molecules, all sharing the same group velocity.

Long-range bound, phase-uncorrelated soliton states[15] are ideal start- and end-points for the synthesis and dissociation of phase-locked soliton molecules. In order to initiate soliton reactions, long-range repulsive forces between solitons must be controlled either globally or individually. As shown in Fig. 1a, global control is achieved mainly by perturbing specific laser parameters, such as pump power, cavity loss, etc (see SI Section I). Abrupt attenuation of long-range repulsive forces within the traps can cause the solitons to move towards each other, resulting in multiple collisions and eventually the formation of a soliton molecule. Conversely, soliton molecules can be broken up by enhancing the repulsive forces, causing the solitons to dissociate and settle down into a phase-uncorrelated long-range bound state (Fig. 1d). Reactions can also be triggered in individual traps by launching addressing pulses into the laser cavity to perturb the soliton interactions by cross-phase modulation (XPM)[14] (see Fig. 1a). Individual control allows each solitonic element to be reversibly and selectively edited (see results below). Thus the optoacoustic traps can host controllable reactions between solitonic elements in a manner reminiscent of chemical reactors (see Fig. 1e).

Results

Synthesis of parallel soliton molecules

To investigate the dynamics of soliton-molecule formation, we prepared a stable soliton supramolecule (see Methods) as the initial state (Fig. 2a), consisting of 195 time-slots, all with two long-range-bound solitons, except for a reference slot containing a single soliton (see Fig. 2b). In the absence of repulsive forces, the solitons within a single time-slot will tend to collide. This is prevented in practice by repulsive forces that arise from the shedding of dispersive waves[5,46,47], leading to formation of a secondary trapping potential (Fig. 1d) that causes long-range binding at ~ 60 ps separation (Figs. 2b and 2c)—much longer that the ~ 1 ps duration of the solitons (see SI Section II). As a result the two trapped solitons have negligible field overlap and are thus uncorrelated in phase[5,15].

Synthesis is initiated by abruptly changing the pump power or the intra-cavity loss, which causes a decrease in the inter-soliton repulsive force (see SI Section II) and a gradual reduction in soliton spacing in all the reactors, culminating in multiple soliton collisions (Fig. 2a). We studied the real-time motion of the reacting solitons by time-domain recording (limited by the bandwidth of the photodiode, so suitable only for long-range binding) and DFT (suitable for short-range (< 14 ps) binding) in all the reactors (see Methods). The entire reaction process over all time-slots, initiated by pump perturbation, was first recorded at 5 kHz frame rate and is shown in Fig. 2b in cylindrical coordinates for 5 selected frames (see Supplementary Movie 1 and SI Section III). Recordings over the initial 49,000 round-trips (~ 5 ms) in 8 consecutive reactors (out of 195) are plotted in Fig. 2c and 2d, showing the soliton dynamics on finer time-scales.

The experimental results indicate that the formation of a stable soliton-pair, resembling a molecule, generally requires multiple collisions within the reactors before an effective collision establish a stable spacing/phase relation between the solitons. As shown in Fig. 2c and Supplementary Movie 1, while in some reactors a stable soliton pair formed within 5 ms after only a few soliton collisions, in many other reactors hundreds of collisions were required. In average, an effective collision occurred out of ~ 25 collisions as we estimate from the recording. To examine the statistics of the synthesis, the cumulative collision numbers in all the reactors is plotted in Fig. 2e against the total number of soliton molecules, measured at time intervals of 50 μs. The plot shows an approximately linear dependence, consistent with the collision theory of chemical kinetics which states that the rate of a gas-phase reaction is proportional to the collision frequency[48]. (See SI Section IV).

Once formed, the soliton molecules would propagate as single entities with precisely synchronized phase and group velocities between the bound solitons. However, they would generally differ[40–42] from single solitons in group velocity, and as a consequence, gradually shift to slightly different positions within their time-slots, while remaining trapped by the optoacoustic trapping potential, as seen in Fig. 2c; see also the reference slot in final state in Fig. 2b. The optomechanical lattice is robust enough to host all the soliton reactions until they are completed, without destabilization.

By retrieving the soliton spacings and phases from the DFT signal[11], the complex nonlinear dynamics after the initiation in hundreds of parallel soliton reactors can be resolved, revealing the stochasticity of soliton-molecule formation (see Fig. 3). Panel (i) – (iii) in Fig. 3a (with corresponding trajectories in Figs. 3b – 3e) show reaction processes in 3 parallel reactors in which the two solitons in each time-slot attempt to transit from a phase-uncorrelated long-range bound state (~ 60 ps spacing) to a phase-locked soliton-molecule (3.8 ps spacing and π-phase difference[22]) after the pump power is perturbed (same as in Fig. 2). While in panel (i) the formation process is completed within 1000 round-trips, following a rather simple trajectory (spacing and phase evolution in Fig. 3b and interaction plane[21] in Fig. 3c), the reaction shown in panel (ii) lasted more than 3000 cavity round-trips and followed a more complex trajectory (see Fig. 3d). Panel (i) and (ii) show how effective collisions could took place in a reactor, while Panel (iii) shows a more frequently observed case of soliton collision which lasts thousands of cavity round-trips without, however, giving birth to a soliton molecule (see Fig. 3e). Instead, the two solitons strongly repel each other, before drifting towards the next collision.

We observed that the soliton motion at most separations is stochastic, reminiscent of a one-dimensional random walk with fixed step-length[49]. This is probably caused by phase-dependent inter-soliton forces[4,19] that are constantly varying in strength and direction, weakly perturbed by non-solitonic components[47]. The initial phase difference between two solitons before binding is also random[15], probably accounting for the widely different trajectories from reactor to reactor. When the soliton separation is less than the molecular spacing (< 3.8 ps), however, a strong repulsive force emerges[4] which quickly pushes the solitons apart. This is a ubiquitous feature not only in the synthesis of soliton-molecules but also in their dissociation, as described below (see SI Section V.). Only in effective collisions, the colliding solitons

would enter a converging trajectory with quickly damped spacing and phase relation (see DFT signal in Fig. 3b and 3d).

Synthesis between different solitonic elements have also been realized in controlled manner using the parallel-reactors, which was previously challenging due to their intrinsic velocity discrepancy that cause uncontrolled collisions. In experiment, we first prepared a soliton supramolecule in which most time-slots hosted a single soliton bound with a soliton-pair molecule, their group velocities being synchronized by long-range interactions[15] such that they would not collide freely before the initiation[45]. Then we abruptly increased the intra-cavity loss using the fast tunable attenuator, which weakened the dispersive-wave perturbation (See SI Section II). Consequently, attraction overcame repulsion, initiating soliton reactions. Two examples of three-soliton reactions are shown in panels (iv) and (v) of Fig. 3a. In panel (iv), collision between the soliton pair and the single soliton resulted in formation of a phase-locked soliton triplet. The measured trajectories between neighbouring solitons during synthesis in panel (iv) are shown in Fig. 3 f. The single soliton collides strongly with the soliton-pair, resulting in strong disturbance to the soliton-pair (highlighted in yellow in Fig. 3f) before the establishment of a second molecular bond (the reaction process is sketched in Fig. 3g). In panel (v), however, a similar collision result in dissociation of the soliton-pair molecule, followed by strong repulsion between all three solitons, highlighting the complexity during the three-soliton reactions. (See SI Section VI)

Dissociation of parallel soliton molecules

Phase-locked soliton molecules can also dissociate into single solitons under global control (Fig. 4a). A typical example is recorded and plotted in cylindrical coordinates in Fig. 4b for 5 selected frames (for full recording see Supplementary Movie 2). The reaction is initiated by a slight decrease in pump power, which enhances the dispersive-wave perturbations, causing rapid break-up of the soliton-molecules. This process is much faster than soliton-molecule formation that generally requires multiple collisions. The dissociation follows highly diverse trajectories from reactor to reactor, as seen in Fig. 4c (time-domain) and Fig. 4d (DFT). We attribute the stochastic fluctuations during the early stages of dissociation to noise-like repulsive forces between the solitons exerted by randomly excited dispersive waves[5,46]. After dissociation, long-range binding between the solitons is gradually established, eventually settling down after a few milliseconds.

Since soliton molecules dissociate over diverse trajectories, the dissociation rate can only be determined statistically. We first define criteria for determining the completion of a reaction: full dissociation for a separation of 14 ps or greater (the maximum spacing retrieved from DFT signal), and long-range soliton binding for a separation of 55 ps or greater. We plot the total number of soliton molecules and long-range double-solitons during dissociation against the number of round-trips (Fig. 4e). Both measurements are roughly exponential, indicating that the dissociation rate is proportional to the number of un-dissociated reactants, i.e. following first-order reaction[48]. This allows us to estimate a soliton-molecule “half-life” of ~ 1200 round-trips (~ 120 μs) using the 14 ps criterion. (See SI Section IV for details)

The soliton motion during dissociation retrieved from the DFT signal are found to share many characteristics with that of synthesis. Figure 5a shows a few dissociation trajectories recorded in the parallel reactors initiated by perturbing the pump power. Panel (i) shows fast dissociation (< 1000 round-trips) with a relatively smooth trajectory, as indicated by the retrieved spacing and phase (Fig. 5b and c). Panel (ii) shows another trajectory recorded within the parallel reactors, which however exhibit a rather long dissociation lasting > 10000 round-trips with a random-walk-like trajectory (see Fig. 5e). Within the trajectory, we can notice a “metastable state” at spacing of ~ 11 ps at which the two solitons temporally reside with quasi-stable relative phases (~ π), which might corresponds to fixed-point attractor with weak stability. Similar phenomena also appeared in other reactors. In addition, we can notice within the trajectory that a strong repulsion[4] occurred (indicated by the blue dashed arrow) when solitons temporally reached a spacing below the initial value (marked by the dashed horizontal line) during the random walk. This phenomenon are found to be universal during the reactions and are also observed in synthesis dynamics (e.g. Figure 3(e)). Such universal soliton repulsion probably result from a mutual frequency shift that occurred spontaneously during significant soliton-overlapping, which quickly flipped their phase relation and turned the inter-soliton force from attraction to repulsion.

In a few reactors, such inter-soliton repulsion can be so radical that the dissociation can terminate immediately. One example is shown in Panel (iii) in Fig. 5) (with DFT signal in Fig. 5e), in which the abrupt drop in soliton spacing triggered strong repulsion between the solitons within only a few round-trips, followed by quick establishment of long-range binding. Occasionally, one (or both) of the interacting solitons are extinguished after such radical repulsion, as shown by the example in panel (iv) of Fig. 5a (with DFT signal in Fig. 5f). This is probably due to the fact that the carrier frequency of both solitons are significantly shifted during the radical repulsion, which affects their gain/loss balance in the laser cavity with limited gain bandwidth. The diverging soliton then experience net loss and failed to recover before the long-range forces (trapping potential) shift the frequency back (See SI Section V for more details.)

Dissociation of soliton-triplets follows even more complex dynamics, as seen when the system is loaded with soliton-triplets in each reactor and then perturbed by decreasing the cavity-loss. Three examples recorded within the parallel reactors are shown in Fig. 6. Panel (i) and (ii) show dissociations that breaks either of the two molecular-bonds within the triplet, leading to different orientations between the soliton pair and the single soliton in the final long-range bound state (see DFT signal in Fig. 6b and c). In panel (iii), both molecular-bonds between the three solitons are severed, resulting in three phase-uncorrelated single solitons (See SI Section VI for more examples.)

All-optical control of soliton reactions in selective reactors

Soliton interactions within selected reactors can be controlled by launching a sequence of precisely timed optical pulses into the laser cavity (Fig. 1a)[12,14,31], permitting individual solitonic elements to be edited by XPM (see Methods and SI Section VII). To demonstrate this, we first prepared a soliton supramolecule in which a mixture of long-range double-solitons and phase-locked soliton-pairs exist in the time-slots. To convert two long-range-bound solitons into a soliton molecule, we launched a train of ~ 200-ps pulses at

the cavity round-trip frequency, precisely timed to interact with targeted time-slots over ~ 3000 round trips (see Fig. 7a and 7b). Since the two solitons initially ride on different amplitude upon each addressing pulse, the two solitons would see different XPM-induced nonlinear index and tend to move closer. Therefore, an effective “attraction force” was applied to the solitons that exceed their long-range repulsion, leading to soliton collisions and formation of stable soliton-molecules (as shown DFT signal and retrieved trajectory in Fig. 7c from selected time-slots). Note that each addressing pulse only accompanied the intra-cavity soliton over a several-meter SMF section before getting absorbed by the intra-cavity polarizer (to prevent laser gain depletion). Therefore, many addressing pulses (typically a few thousands) are required to be launch repetitively to the same time-slot to ensure sufficient overlapping time with the solitons (See SI Section VII for details).

Conversely, to break apart soliton molecules in selected reactors, we developed a special trick that made use of the same train of addressing pulses as above with however a slight offset in repetition rate. In this case, the addressing pulses would effectively “walk through” the soliton molecule and impose a mutual frequency shift through a time-domain varying XPM [50] (see Fig. 7d). The externally-induced frequency-shift would flip the phase-relation of the soliton molecule from π to 0, causing strong attraction and thus compressed spacing. Then a following frequency-shift is triggered (similar to the case in Fig. 5e), which flipped the phase-relation and thus the force direction back, leading to radical repulsion that pushed the solitons apart. The addressing pulses in this case operate like an optical “scissors”, severing the molecular bond while traversing. By suitable choice of repetition-rate offset ($f_{ext} - f_{cav} \approx 20$ Hz, see Fig. 7e), we achieved deterministic dissociation of selected soliton-molecules. The trajectories retrieved from the DFT signal are shown in Fig. 7f, revealing that the traversing pulse first compresses the soliton separation to below ~ 5 ps, triggering strong repulsion within 2 ~ 3 round trips, and eventually leading to the collapse of the molecular bond and establishment of long-range binding (See SI Section VII for details).

Discussion And Conclusion

The parallel-reactor scheme makes it possible to extract a massive amount of soliton-dynamic events out of each initiation, from which we have revealed a series of stochastic features with abundant instances. During the synthesis and dissociation of soliton molecules, the interacting solitons follow a random-walk-like motions that are highly diverse over different reactors, probably as a results of phase-sensitive interactions. Meanwhile, the interacting solitons could temporally reside on some “metastable states” with quasi-stable spacings and phase relations. Moreover, strong soliton repulsions occurred, as we observed, whenever the soliton spacings reached below the molecular spacing, which could hinder the formation of soliton molecule during synthesis or radically severe the soliton-molecular bond during the dissociation.

Despite the stochasticity within each individual soliton interactions, simple statistical rules are found out of surprise that govern soliton reactions at a collective level. Multiple collisions are found to be essential for soliton molecule synthesis, while the rate of molecule formation depends linearly on the rate of soliton

collisions over all reactors. The rate of dissociation, on the other hand, are found to be proportional to number of remaining soliton molecules, following first-order reaction model. Both statistical rules highly resemble their counterpart in classical theory of chemical kinetics, offering collective-level light-matter analogy in contrast to previous studies that plateaued at single-entity level.

Compared with other platforms commonly used in the study of soliton dynamics, such as microresonators[8,9,13,29], passive fibre loops[31,38], and solid-state mode-locked lasers[11,12], optoacoustically mode-locked fibre lasers[14] offer several advantages, including high flexibility and simple configuration with no need of external driving or feedback control. The long fibre cavity dissected by the self-organized optomechanical lattice not only accommodate large number of solitons (with possibility of further expansion using longer cavity), but also tolerate the group velocity discrepancies between different solitonic elements, leading to well-isolated and fully-manipulated parallel soliton reactions for the first time. The regular time grid inscribed by acoustic vibrations in PCF also facilitate the precise access to individual reactors using external addressing pulses and thus the studies on responses of soliton complexes to external perturbations.

In addition to the soliton molecule dynamics studied in this work, this system could also be used to re-examine phenomena such as soliton explosions[51], pulsation[34,52], fragmentation[24,52], resonant vibrations[12,33], as well as the build-up[27] and extinction[25] of solitons from a collective viewpoint. As well as permitting a higher-level exploration of the multi-soliton dynamics, the parallel reactor scheme and the new findings on soliton interactions may lead to novel applications in all-optical information processing using solitons as data-bits, e.g. all-optical logic gate[3], non-binary bit-storage[14] and transmission[30].

Methods

Preparing soliton-supramolecule states. In order to generate the desired soliton supramolecule state, we need to choose proper working point for the laser, adjusting the pump power level, cavity loss and most importantly carefully aligning the intra-cavity polarisation controllers. Sometimes dispersion compensating fibres are needed in the cavity to properly tailor the dispersive waves. In addition to the fast tunable optical attenuator, a manual tunable attenuator was also inserted in the cavity to introduce a loss-bias—crucial for finding a proper working point for the parallel reactions.

Soliton sequences plotted in cylindrical coordinates. The soliton sequence propagating in the laser ring-cavity follows a regular time-grid, each time-slot hosting one or more solitons. To simultaneously illustrate the soliton dynamics within all time-slots from frame to frame, we converted the temporal position $\tau_k(n)$ of the k-th soliton in the n-th time-slot into cylindrical coordinates following the relationship $(\rho_k(n), \phi_k(n)) = (\tau_0 + \tau_k(n), n2\pi/N)$, where τ_0 is an arbitrary constant and $N = 195$ is the total number of time-slots (see Figs.2b and 4b). In each azimuthal “slice”, the amplitudes of each soliton are indicated by a colormap. When a soliton sequence consists of soliton molecules, the limited bandwidth of the PD would translate the soliton-pair (or triplet) structure into a single pulse with doubled (or tripled) amplitude compared with that of a single-soliton.

Diagnostic set-up and capacity. We used a 33-GHz bandwidth PD for time-domain measurements, together with a 100 Gbits/s oscilloscope. This yielded a temporal resolution is ~15 ps, with a maximum recording time-span of 2.5 ms that was limited by the oscilloscope memory. To reach longer recording times (5 ms), in a few cases (e.g. in Figs.2b-d and Fig.7b) we reduced the bandwidth to 16 GHz (50 Gbits/s sampling rate). For similar reasons the recordings in Fig.2b and Fig.4b were at different frame rates (5 kHz and 20 kHz), using the oscilloscope to take discrete shots of the round-trip signal during synthesis and dissociation. The DFT signal is obtained by using a 3-km SMF-28 with a GVD of −22.5 ps^2/km (D = +17.65 ps/km/nm) and detected with a 25-GHz PD, corresponding to spectral resolution $\delta\lambda_{res} = 1/(B|D|z) \approx 0.7$ nm at 1.55 μm wavelength, in which B is the PD bandwidth, D is the fibre dispersion, and the z is the fibre length. The optical bandwidth retrieved from the DFT signal is $\Delta\nu$ ~12.5 THz or a $\Delta\lambda$ ~10 nm given by $\Delta\lambda = T/(|D|z)$, in which T is the span of the time-slot. The maximum soliton spacing that can be retrieved by numerical fitting of the DFT signal is ~14 ps, which is limited by the PD bandwidth and the stretching ratio. The precision of the retrieve soliton spacing is affected by the signal to noise ratio of the PD and the intrinsic timing jitter of the oscilloscope. Given ~2 ps uncertainty in the fringe period of interferometric DFT signal, the precision of the retrieved soliton spacing should be < 0.1 ps (for typical soliton spacing around ~10 ps).

External addressing pulses. The addressing pulses launched into the laser cavity were generated by modulating a single-wavelength laser at 1550 nm using a programmable pulse-sequence generator (~200 ps duration). The programmed pulse sequence followed a time grid that exactly matched the optomechanical lattice in the laser cavity, with 256 time-slots and repeated at ~7.344 MHz (laser-cavity length different from that under global control), in order to precisely overlap with selected time-slots. Ten evenly-spaced slots within the programmed time-grid were filled with addressing pulses, which were then amplified to ~ 20 W peak power in two amplifier stages. Launching of the addressing pulse was controlled by an optical switch (20-dB extinction ratio and 100 ns edge-time). The input port was a 50/50 coupler, which was also used as an output coupler. The polarisation state of the addressing pulses was adjusted so that they could be blocked by a polariser after exiting the cavity. In order to obtain a clean DFT signal without overlap from the addressing pulses, we inserted a 90/10 output coupler before the 50/50 output coupler.

Data availability: The data that support the plots within this paper and other findings of this study are available from the corresponding authors upon reasonable request.

Code availability: The code used in this paper is available from the corresponding author upon reasonable request.

Declarations

Acknowledgements

The Max Planck Society is acknowledged for financial support.

Additional Author information

The present address of Meng Pang is State Key Laboratory of High Field Laser Physics, Shanghai Institute of Optics and Fine Mechanics, Chinese Academy of Sciences, Shanghai, 201800, China

Competing interests:

Authors declare no competing interests.

Additional information

Supplementary Information (Sections I – VII), Supplementary Movie 1–2.

Data availability

The data that support the plots within this paper and other findings of this study are available from the corresponding authors upon reasonable request.

Code availability

The code used in this paper is available from the corresponding author upon reasonable request.

Author contributions:

The concept was proposed by W.H., M.P., and P.R., the experiments were carried out by W.H., D.H.Y., and J.H., the results were analysed by W.H. and M.P., and the paper was written by all authors.

References

1. Mollenauer, L. F., Stolen, R. H. & Gordon, J. P. Experimental observation of picosecond pulse narrowing and solitons in optical fibers. *Phys. Rev. Lett.* **45**, 1095–1098 (1980).
2. Haus, H. A. & Wong, W. S. Solitons in optical communications. *Rev. Mod. Phys.* **68**, 423–444 (1996).
3. Islam, M. N., Soccolich, C. E. & Gordon, J. P. Ultrafast digital soliton logic gates. *Opt. Quantum Electron.* **24**, S1215–S1235 (1992).
4. Mitschke, F. M. & Mollenauer, L. F. Experimental observation of interaction forces between solitons in optical fibers. *Opt. Lett.* **12**, 355–357 (1987).
5. Smith, K. & Mollenauer, L. F. Experimental observation of soliton interaction over long fiber paths: discovery of a long-range interaction. *Opt. Lett.* **14**, 1284–1286 (1989).

6. Goda, K. & Jalali, B. Dispersive Fourier transformation for fast continuous single-shot measurements. *Nat. Photon.* **7**, 102–112 (2013).
7. Herr, T. *et al.* Temporal solitons in optical microresonators. *Nat. Photon.* **8**, 145–152 (2014).
8. Yi, X., Yang, Q.-F., Yang, K. Y. & Vahala, K. Imaging soliton dynamics in optical microcavities. *Nat. Commun.* **9**, 3565 (2018).
9. Weng, W., Bouchand, R. & Kippenberg, T. J. Formation and Collision of Multistability-Enabled Composite Dissipative Kerr Solitons. *Phys. Rev. X* **10**, 21017 (2020).
10. Grelu, P. & Akhmediev, N. Dissipative solitons for mode-locked lasers. *Nat. Photon.* **6**, 84–92 (2012).
11. Herink, G., Kurtz, F., Jalali, B., Solli, D. R. & Ropers, C. Real-time spectral interferometry probes the internal dynamics of femtosecond soliton molecules. *Science* **356**, 50–54 (2017).
12. Kurtz, F., Ropers, C. & Herink, G. Resonant excitation and all-optical switching of femtosecond soliton molecules. *Nat. Photon.* **14**, 9–13 (2020).
13. Cole, D. C., Lamb, E. S., Del'Haye, P., Diddams, S. A. & Papp, S. B. Soliton crystals in Kerr resonators. *Nat. Photon.* **11**, 671–676 (2017).
14. Pang, M., He, W., Jiang, X. & Russell, P. St.J. All-optical bit storage in a fibre laser by optomechanically bound states of solitons. *Nat. Photon.* **10**, 454–458 (2016).
15. He, W. *et al.* Formation of optical supramolecular structures in a fibre laser by tailoring long-range soliton interactions. *Nat. Commun.* **10**, 5756 (2019).
16. Wang, Z. Q., Nithyanandan, K., Coillet, A., Tchofo-Dinda, P. & Grelu, P. Optical soliton molecular complexes in a passively mode-locked fibre laser. *Nat. Commun.* **10**, 830 (2019).
17. Tang, D. Y., Man, W. S., Tam, H. Y. & Drummond, P. D. Observation of bound states of solitons in a passively mode-locked fiber laser. *Phys. Rev. A* **64**, 33814 (2001).
18. Herink, G., Kurtz, F., Jalali, B., Solli, D. R. & Ropers, C. Real-time spectral interferometry probes the internal dynamics of femtosecond soliton molecules. *Science* **356**, 50–54 (2017).
19. Gordon, J. P. Interaction forces among solitons in optical fibers. *Opt. Lett.* **8**, 596–598 (1983).
20. Malomed, B. A. Bound solitons in the nonlinear Schrodinger-Ginzburg-Landau equation. *Phys. Rev. A* **44**, 6954–6957 (1991).
21. Akhmediev, N. N., Ankiewicz, A. & Soto-Crespo, J. M. Stable soliton pairs in optical transmission lines and fiber lasers. *J. Opt. Soc. Am. B* **15**, 515–523 (1998).
22. Afanasjev, V. V. & Akhmediev, N. Soliton interaction and bound states in amplified-damped fiber systems. *Opt. Lett.* **20**, 1970–1972 (1995).
23. Krupa, K., Nithyanandan, K., Andral, U., Tchofo-Dinda, P. & Grelu, P. Real-Time Observation of Internal Motion within Ultrafast Dissipative Optical Soliton Molecules. *Phys. Rev. Lett.* **118**, 243901 (2017).
24. Liu, X., Yao, X. & Cui, Y. Real-Time Observation of the Buildup of Soliton Molecules. *Phys. Rev. Lett.* **121**, 23905 (2018).
25. Peng, J. & Zeng, H. Build-Up of Dissipative Optical Soliton Molecules via Diverse Soliton Interactions. *Laser Photon. Rev.* **12**, 1800009 (2018).

26. Shi, H., Song, Y., Wang, C., Zhao, L. & Hu, M. Observation of subfemtosecond fluctuations of the pulse separation in a soliton molecule. *Opt. Lett.* **43**, 1623–1626 (2018).
27. Herink, G., Jalali, B., Ropers, C. & Solli, D. R. Resolving the build-up of femtosecond mode-locking with single-shot spectroscopy at 90-MHz frame rate. *Nat. Photon.* **10**, 321–326 (2016).
28. Kerse, C. *et al.* Ablation-cooled material removal with ultrafast bursts of pulses. *Nature* **537**, 84–88 (2016).
29. Weng, W. *et al.* Heteronuclear soliton molecules in optical microresonators. *Nat. Commun.* **11**, 2402 (2020).
30. Rohrmann, P., Hause, A. & Mitschke, F. Solitons Beyond Binary: Possibility of Fibre-Optic Transmission of Two Bits per Clock Period. *Sci. Rep.* **2**, 866 (2012).
31. Leo, F. *et al.* Temporal cavity solitons in one-dimensional Kerr media as bits in an all-optical buffer. *Nat. Photon.* **4**, 471–476 (2010).
32. Churkin, D. V *et al.* Stochasticity, periodicity and localized light structures in partially mode-locked fibre lasers. *Nat. Commun.* **6**, 7004 (2015).
33. Ryczkowski, P. *et al.* Real-time full-field characterization of transient dissipative soliton dynamics in a mode-locked laser. *Nat. Photon.* **12**, 221–227 (2018).
34. Soto-Crespo, J. M., Akhmediev, N. & Ankiewicz, A. Pulsating, Creeping, and Erupting Solitons in Dissipative Systems. *Phys. Rev. Lett.* **85**, 2937–2940 (2000).
35. Solli, D. R., Ropers, C., Koonath, P. & Jalali, B. Optical rogue waves. *Nature* **450**, 1054–1057 (2007).
36. Tang, D. Y., Zhao, B., Zhao, L. M. & Tam, H. Y. Soliton interaction in a fiber ring laser. *Phys. Rev. E* **72**, 16616 (2005).
37. Turaev, D., Vladimirov, A. G. & Zelik, S. Chaotic bound state of localized structures in the complex Ginzburg-Landau equation. *Phys. Rev. E* **75**, 45601 (2007).
38. Jang, J. K., Erkintalo, M., Murdoch, S. G. & Coen, S. Ultraweak long-range interactions of solitons observed over astronomical distances. *Nat. Photon.* **7**, 657–663 (2013).
39. Kodama, Y., Wabnitz, S. & Romagnoli, M. Soliton stability and interactions in fibre lasers. *Electron. Lett.* **28**, 1981–1983 (1992).
40. Roy, V., Olivier, M., Babin, F. & Piché, M. Dynamics of Periodic Pulse Collisions in a Strongly Dissipative-Dispersive System. *Phys. Rev. Lett.* **94**, 203903 (2005).
41. Weng, W., Bouchand, R., Lucas, E. & Kippenberg, T. J. Polychromatic Cherenkov Radiation Induced Group Velocity Symmetry Breaking in Counterpropagating Dissipative Kerr Solitons. *Phys. Rev. Lett.* **123**, 253902 (2019).
42. Akhmediev, N., Soto-Crespo, J. M., Grapinet, M. & Grelu, P. Dissipative soliton interactions inside a fiber laser cavity. *Opt. Fiber Technol.* **11**, 209–228 (2005).
43. Kang, M. S., Nazarkin, A., Brenn, A. & Russell, P. St.J. Tightly trapped acoustic phonons in photonic crystal fibres as highly nonlinear artificial Raman oscillators. *Nat. Phys.* **5**, 276–280 (2009).
44. Liu, L. R. *et al.* Building one molecule from a reservoir of two atoms. *Science* **360**, 900–903 (2018).

45. Grelu, P. & Akhmediev, N. Group interactions of dissipative solitons in a laser cavity: the case of 2 + 1. *Opt. Express* **12**, 3184–3189 (2004).
46. Noske, D. U., Pandit, N. & Taylor, J. R. Source of spectral and temporal instability in soliton fiber lasers. *Opt. Lett.* **17**, 1515–1517 (1992).
47. Loh, W. H., Afanasjev, V. V., Payne, D. N. & Grudinin, A. B. Soliton interaction in the presence of a weak nonsoliton component. *Opt. Lett.* **19**, 698–700 (1994).
48. Connors, K. A. *Chemical Kinetics: The Study of Reaction Rates in Solution*. (Wiley, 1990).
49. Franz, A., Seeger, S., Hoffmann, K. H. & Schulzky, C. Diffusion on Fractals — Efficient algorithms to compute the random walk dimension, in *Fractal Geometry*. 52–67 (Elsevier, 2002).
50. Islam, M. N., Menyuk, C. R., Chen, C.-J. & Soccolich, C. E. Chirp mechanisms in soliton-dragging logic gates. *Opt. Lett.* **16**, 214–216 (1991).
51. Runge, A. F. J., Broderick, N. G. R. & Erkintalo, M. Observation of soliton explosions in a passively mode-locked fiber laser. *Optica* **2**, 36–39 (2015).
52. Huang, J., Pang, M., Jiang, X., He, W. & Russell, P. St.J. Route from single-pulse to multi-pulse states in a mid-infrared soliton fiber laser. *Opt. Express* **27**, 26392–26404 (2019).

Figures

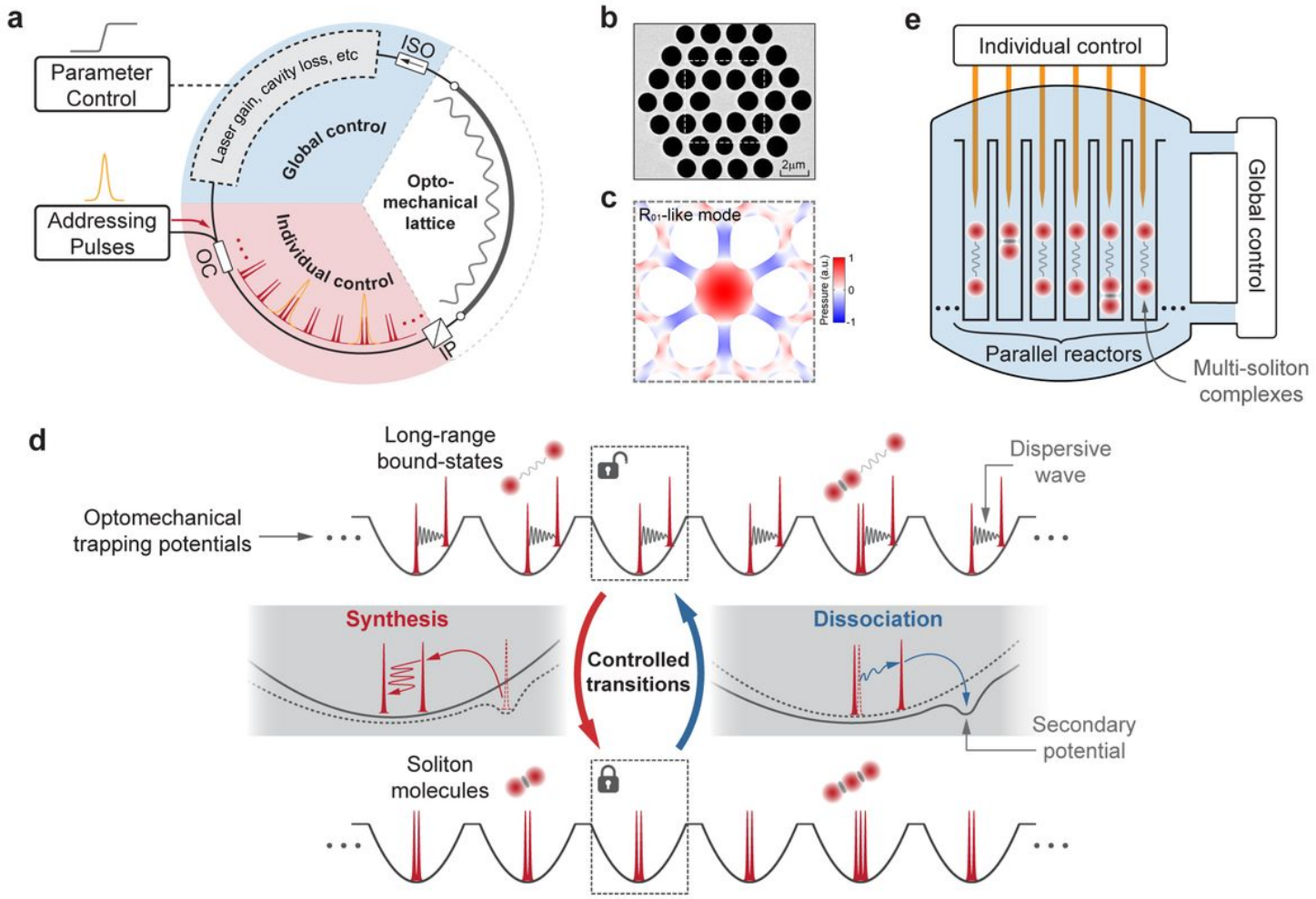

Figure 1

Conceptual illustration of parallel optical-soliton reactors in a fibre laser cavity. a Schematic of the mode-locked fibre laser cavity. IP: inline polariser, OC: optical coupler, ISO: isolator. The acoustic resonance in the PCF core creates an optomechanical lattice that divides the laser cavity into many separate time-slots, each hosting a few solitons. In order to initiate soliton reactions in these time-slots, the laser parameters can be perturbed globally or by addressing individual time-slots with carefully timed external pulses. b Scanning electron micrograph (SEM) of the PCF microstructure. c Finite-element simulation of the R01-like acoustic mode in the PCF core. The displacement is exaggerated for clarity and the normalized pressure is indicated by the colour map. d Schematic of controlled soliton reactions in the optomechanical lattice. The solitonic elements trapped in each reactor can be transitioned between phase-uncorrelated long-range bound states and phase-locked soliton molecules, corresponding to the synthesis and dissociation of soliton molecules. e Sketch of a system of parallel soliton reactors with global and individual control, mimicking a chemical reactor.

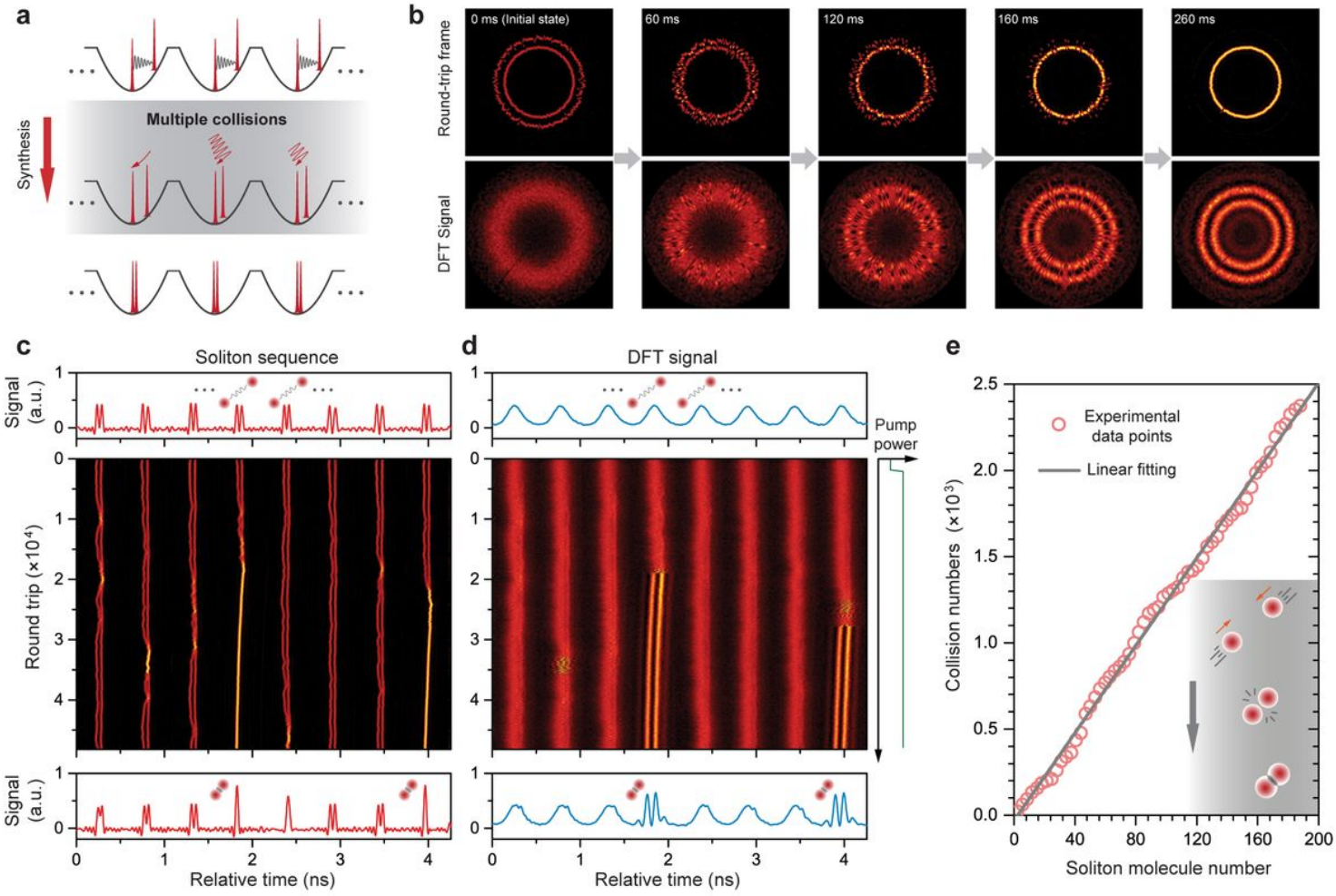

Figure 2

Global synthesis of phase-locked soliton molecules. a Schematic of the synthesis of soliton molecules in parallel reactors. Two solitons are initially prepared in a long-range phase-uncorrelated bound state. After an abrupt change in pump power or cavity loss, the long-range binding collapses and the two solitons experience multiple collisions before forming a stable soliton molecule. b Upper row: Selected frames from an experimental recording of the synthesis process over all 195 reactors, plotted in cylindrical coordinates (see Methods). Lower: The corresponding DFT signal. The initial state contains 194 time-slots with two long-range bound solitons and a reference time-slot with a single soliton. The gradual establishment of spectral fringes in the DFT signal in all time-slots indicates formation of soliton molecules. See Supplementary Movie 1 for the complete recording. c Time-domain evolution in 8 consecutive time-slots over the initial 49,000 round-trips (~5 ms). d The corresponding DFT signal. Soliton molecules have formed in only two time-slots, as indicated by the sharp fringes in d. Top and bottom panels in c and d show the recorded signals for the initial and final round-trips. e Cumulative number of soliton collisions is proportional to the number of soliton molecules in all 195 reactors during a single synthesis (red circles). The grey line is a linear fit.

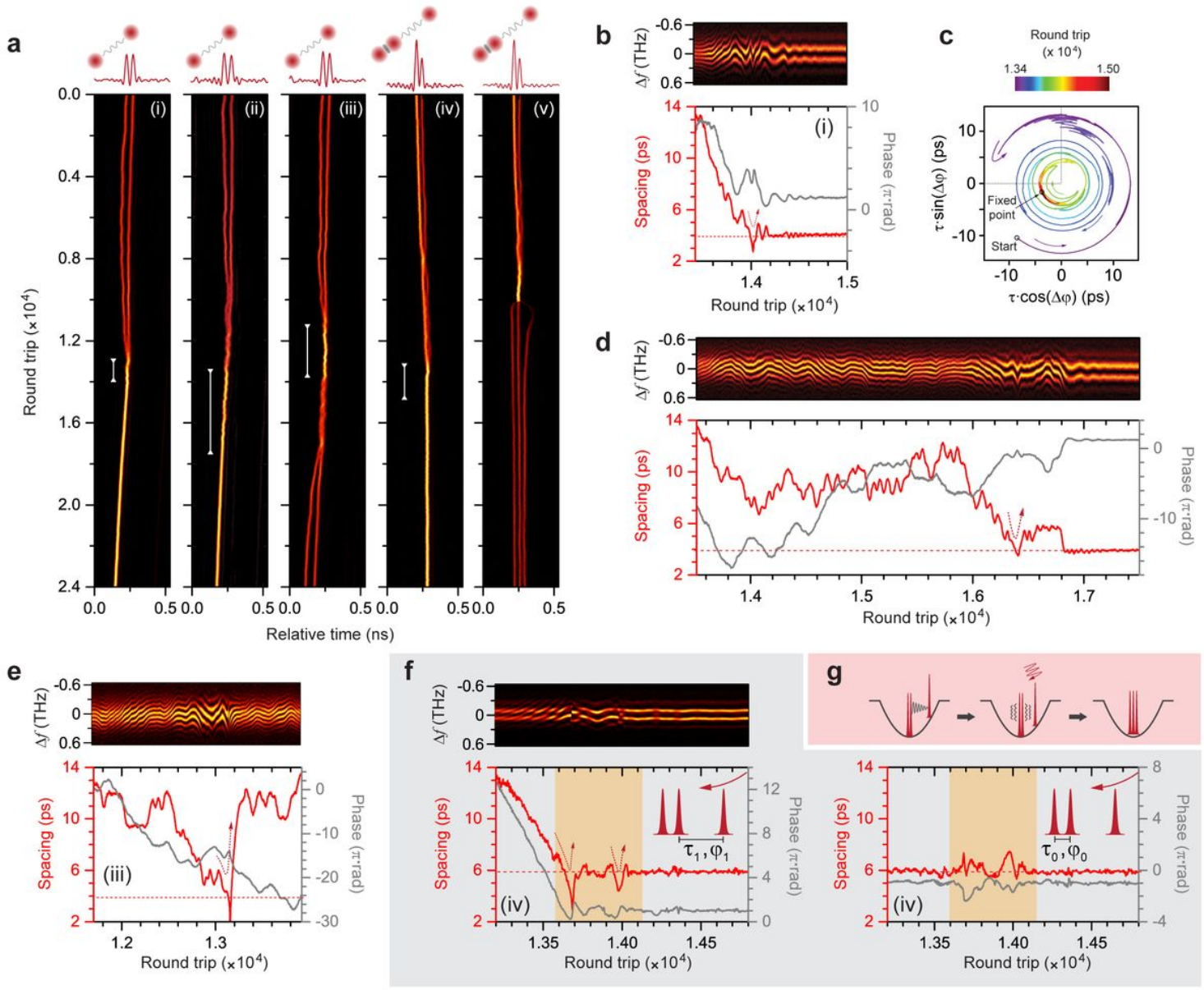

Figure 3

Dissociation of soliton molecules in parallel reactors. a Schematic of the dissociation process in the case when all the reactors contain identical soliton molecules. By perturbing the pump power or the cavity loss, the molecular bonds collapse and the solitons start to drift stochastically and diverge, before reaching a stable long-range bound state. b Upper panels: selected frames from experimental measurements of the dissociation process in all 195 reactors, plotted in cylindrical coordinates. Lower panels: the corresponding DFT signals. Initially all the time-slots are occupied by identical soliton molecules with spacings of ~3.8 ps and a relative phase of ~π. The gradual smearing-out of interferometric fringes in the DFT signal indicates dissociation. See Supplementary Movie 2 for the complete recording. c, d Time-domain sequence in 8 consecutive time-slots over the first 16000 round-trips (~1.8 ms) and the corresponding DFT signal, exhibiting instant collapse of the molecular bonds following pump-power perturbation. The dissociation trajectories are highly diverse, as indicated by fringes in d. Upper and lower panels in c and d show the signal traces for the initial and final round-trips. e Populations of soliton

molecules (red squares) and long-range double-solitons (blue circles) over all 195 reactors, plotted against round-trip number during dissociation, fitted to exponential functions (grey curves). The horizontal dashed line marks the perturbation time.

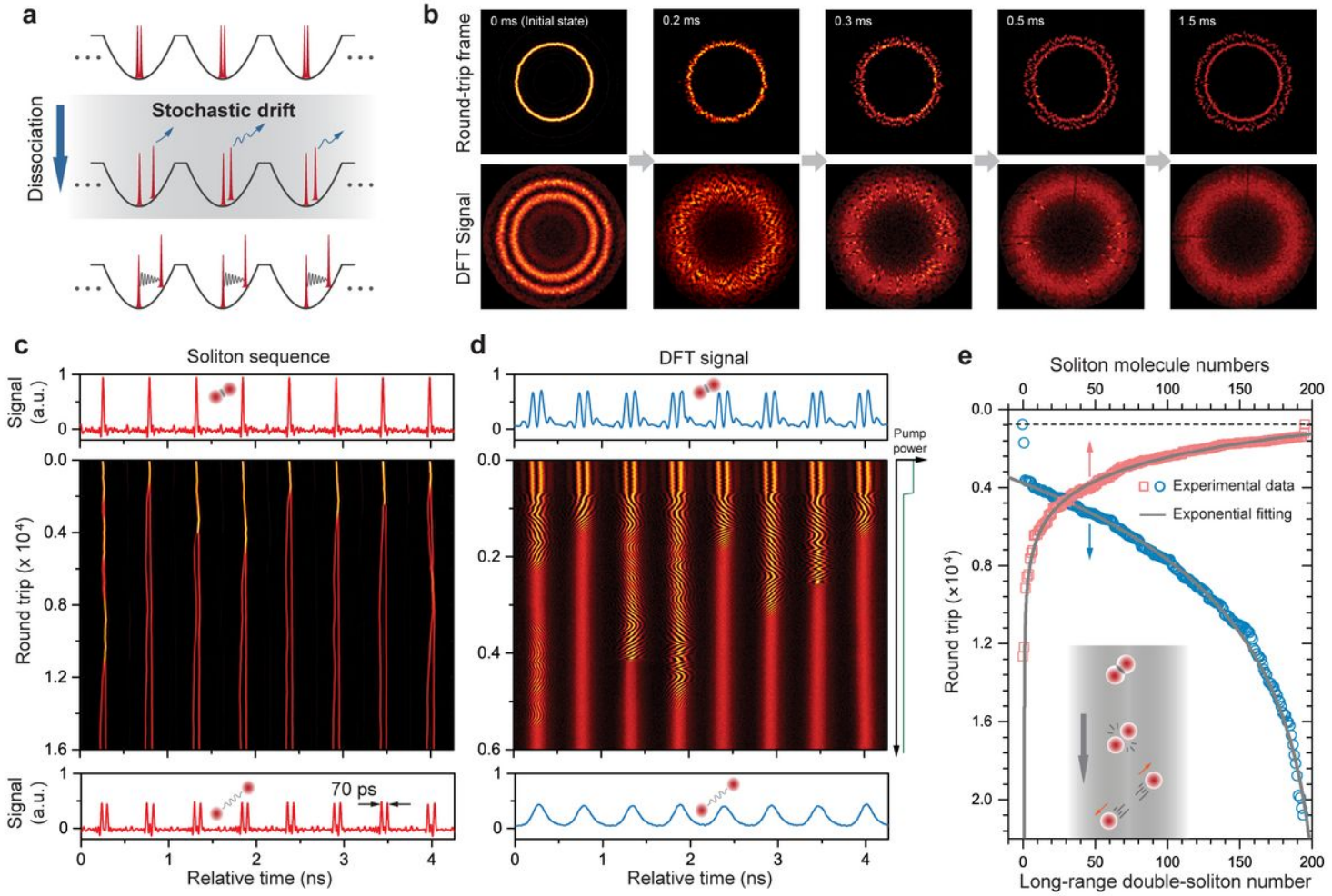

Figure 4

Dissociation of soliton molecules in parallel reactors. a Schematic of the dissociation process in the case when all the reactors contain identical soliton molecules. By perturbing the pump power or the cavity loss, the molecular bonds collapse and the solitons start to drift stochastically and diverge, before reaching a stable long-range bound state. b Upper panels: selected frames from experimental measurements of the dissociation process in all 195 reactors, plotted in cylindrical coordinates. Lower panels: the corresponding DFT signals. Initially all the time-slots are occupied by identical soliton molecules with spacings of ~3.8 ps and a relative phase of ~π. The gradual smearing-out of interferometric fringes in the DFT signal indicates dissociation. See Supplementary Movie 2 for the complete recording. c, d Time-domain sequence in 8 consecutive time-slots over the first 16000 round-trips (~1.8 ms) and the corresponding DFT signal, exhibiting instant collapse of the molecular bonds following pump-power perturbation. The dissociation trajectories are highly diverse, as indicated by fringes in d. Upper and lower panels in c and d show the signal traces for the initial and final round-trips. e Populations of soliton molecules (red squares) and long-range double-solitons (blue circles) over all 195 reactors, plotted

against round-trip number during dissociation, fitted to exponential functions (grey curves). The horizontal dashed line marks the perturbation time.

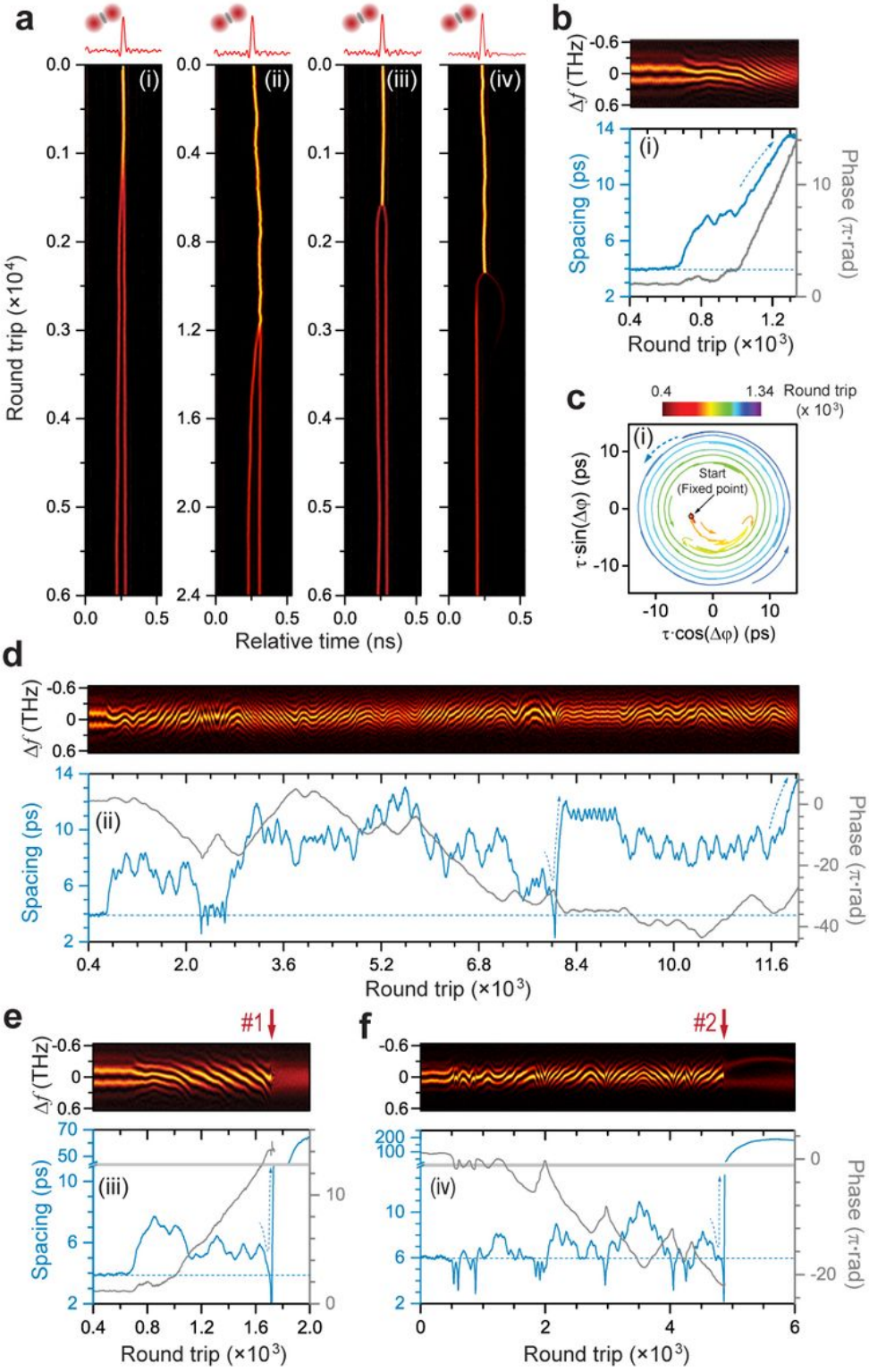

Figure 5

Dissociation dynamics of soliton-pair molecules. a Time-domain recordings in three selected time-slots showing reactions of long-range bound solitons (~ 60 ps spacing) into soliton-pair molecules (~ 3.8 ps inner spacing). Panels (i) and (ii) show successful synthesis, while panel (iii) shows dissociation after

collision. b - e DFT-signal (upper) and retrieved spacing and phase evolution (lower) for the ranges marked by white lines in panels (i) - (iii) (c is the interaction-plane plot of b). The horizontal dashed lines mark the spacing of a stable molecule. The horizontal dashed-lines mark the minimum soliton spacing (~ 6 ps) in the final state.

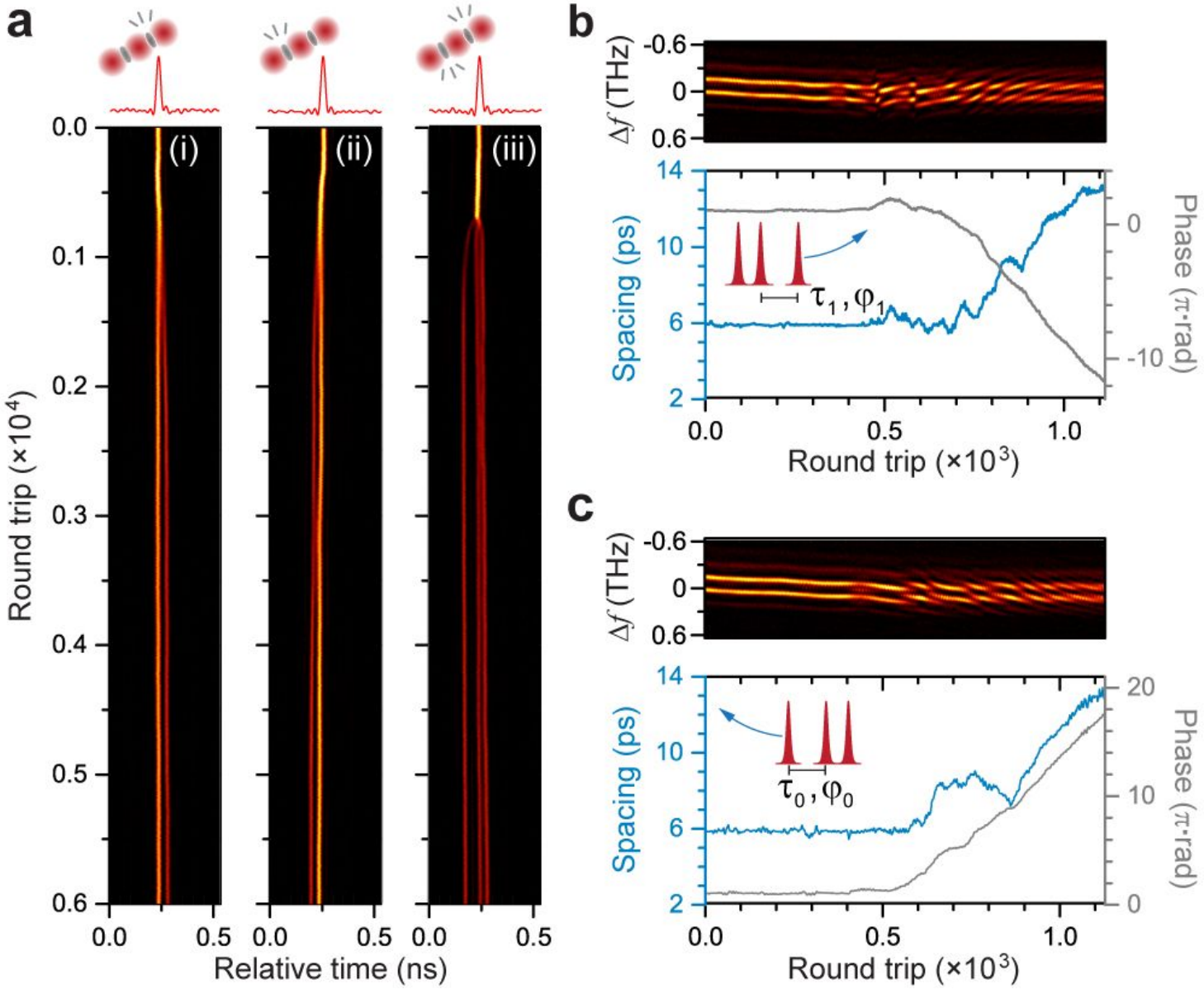

Figure 6

Dissociation dynamics of soliton-triplet molecules. a Time-domain recordings of soliton-triplet dissociation in three selected reactors. In panel (i) and (ii), the dissociation breaks either of the two molecular-bonds, resulting in a soliton-pair molecule and a single soliton with different orders. The corresponding DFT signal are shown in b and c. In panel (iii), both molecular-bonds are severed, resulting in three uncorrelated solitons.

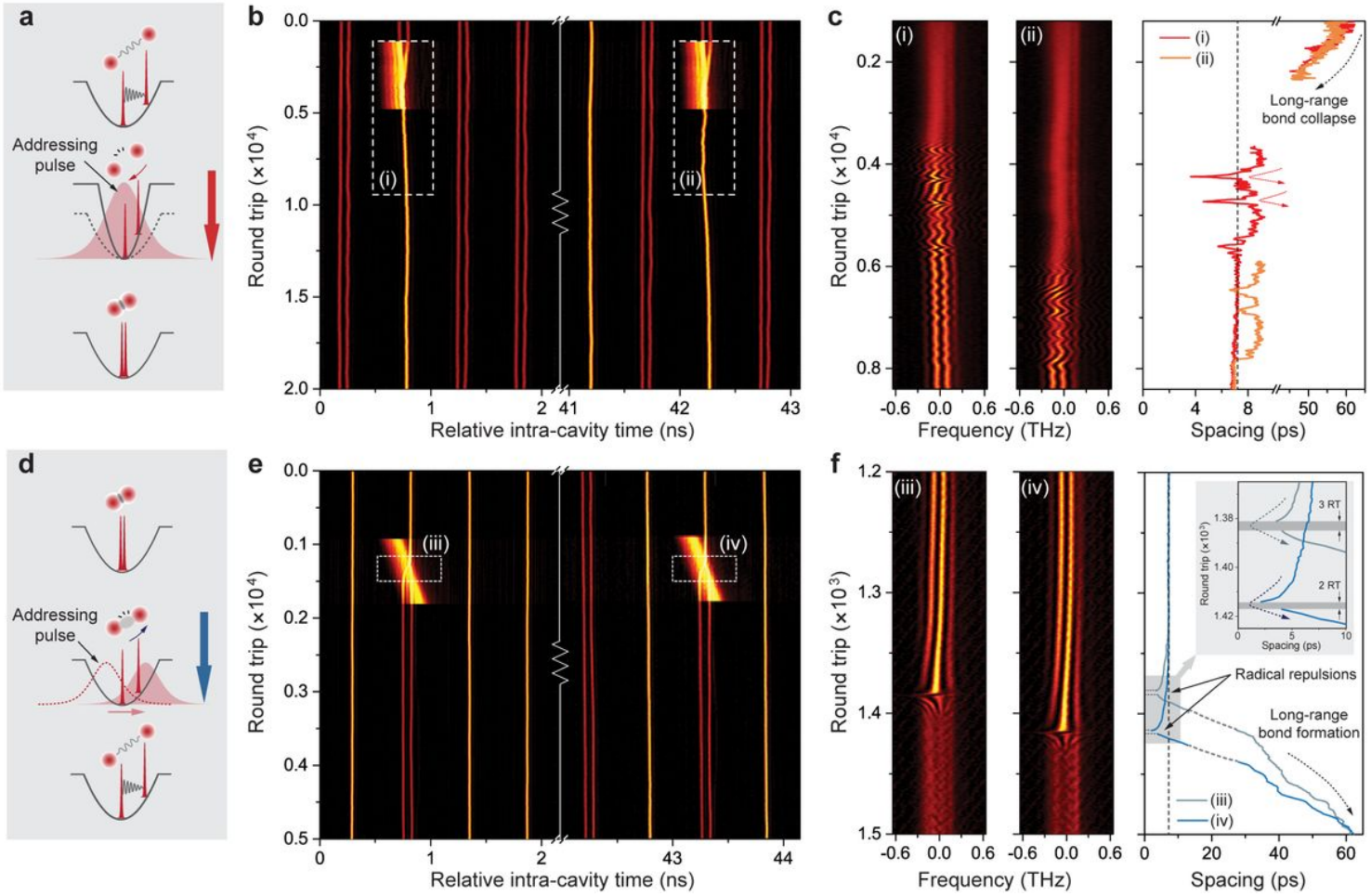

Figure 7

Control of reactions in selected time-slots by external pulses. a An external addressing pulse overlaps continuously with an initially-prepared long-range soliton pair, causing strong attractive forces between them that result in formation of a soliton molecule. b Time-domain recordings of two processes in reactors hosting long-range soliton pairs. A 200-ps-long addressing pulse overlaps with the solitons over ~3000 round trips, causing the two solitons to drift together, interact, and form a soliton molecule. c DFT signals of the interaction within the white dashed boxes (i) and (ii) in b, together with the evolution of the inter-soliton spacing. d Schematic of soliton-molecule dissociation by an external addressing pulse. The addressing pulse traverses the soliton molecule, quickly severing the molecular bond. The two dissociated solitons become long-range bound in the end. e Time-domain recordings of the dissociation processes in reactors containing soliton-pairs. Addressing pulses with a slight repetition-rate offset “sweep” across the soliton molecules over 200 round trips, causing breakage of the soliton-molecule, followed by the establishment of long-range binding. f DFT signal for the processes within the white dashed boxes (iii) and (iv) in e, together with the evolution of the inter-soliton spacing. Strong repulsion is observed during dissociation when the spacing falls below ~5 ps, which occurred within 2~3 round trips, as shown in the inset.

Supplementary Files

This is a list of supplementary files associated with this preprint. Click to download.

- Video1Synthesis.mov
- Video2Dissociation.mov
- HeParallelreactorsSupple20200809.pdf